THE JOURNAL OF EXPERIMENTAL ZOOLOGY 268:307–322 (1994)

Endogenous Ionic Currents and Voltages in Amphibian Embryos

M.E. MOUREY METCALF, RIYI SHI, AND RICHARD B. BORGENS
Center for Paralysis Research, Department of Anatomy, School of Veterinary Medicine, Purdue University, West Lafayette, Indiana 47907–1244

ABSTRACT Using a noninvasive vibrating electrode for the measurement of extracellular current, we show that a polarized ionic current traverses the embryo for many hours in the anuran, perhaps days in the urodele following gastrulation. The voltage driving these ionic currents is an internally positive transepithelial potential (TEP) normally expressed across embryonic integuments. Current is driven out of the lateral walls of the neural folds and the blastopore and enters most of the rest of the embryo's body surface. The magnitude of the TEP is transitorily dependent on external sodium and can be reduced by the embryo's immersion in Na^+ depleted media or by treatment with 50 μM amiloride. Both treatments fail to chronically reduce externally detected currents, however. The pattern of currents traversing the embryo suggests they would be associated with rostral-caudal and medial-lateral gradients of voltage within the embryo. By sampling the distribution of TEPs in axolotl embryos, we provide measurements of the former—an internal, caudally negative, potential gradient beneath the neural plate ectoderm. The magnitude of these endogenous fields is on the order of 10 to 20 mV/mm and is within a range of potential known to affect the shape and migration of a variety of embryonic cell types in vitro. We suggest that endogenous currents and voltages in the vertebrate embryo may provide gross cues for cell movement and emerging developmental pattern.

It is not commonly appreciated that steady, polarized DC currents are driven through developing animals and plants for hours, even days. These endogenous ionic currents (and their associated voltage gradients) may be controls of development and not accidental to it (Jaffe and Nuccitelli, '77; Borgens et al., '79a; Jaffe, '81, '82). Endogenous currents often foreshadow the locus of cell growth, orientation, or migration. For example, the precise location where embryonic limb buds will form is predicted by an outward flow of ionic current (taken to be the direction in which positive charge moves) in both *Xenopus laevis* (Robinson, '83) and *Ambystoma mexicanum* (Borgens et al., '83). The associated subepidermal voltage gradient (negative beneath the region of outwardly directed current) has been proposed to serve as a coarse guide for the accumulation of limb bud mesenchyme as well as subsequent projections of axons (Borgens, '84, '89). The migration of mobile embryonic cell types such as neural crest cells (Stump and Robinson, '83; Cooper and Keller, '84), embryonic fibroblasts (Nuccitelli and Erickson, '83; Erickson and Nuccitelli, '84), and projections of embryonic *Xenopus* neurites (Hinkle et al., '81; McCaig, '87; Borgens and McCaig, '89) toward the cathode of an applied electric field is consistent with such a hypothesis. Furthermore, discontinuities in the pattern or polarity of transcellular or transembryonic ion currents have been postulated to be the physiological basis for discontinuity in positional values leading to change in developing symmetry and pattern formation (Jaffe, '81). Though circumstantial evidence for an electrical control of development is extensive, there has been little direct evidence for causality.

In amphibian embryos, weak ionic currents with densities of a few $\mu A/cm^2$ can be detected entering most of their surface. This is associated with a uniform uptake of Na^+ from the dilute environment. This electrogenic inward Na^+ transport produces an internally positive transepithelial potential (TEP) that develops across the embryonic integument (McCaig and Robinson, '82; Borgens, '89). This TEP, observed early in embryonic life, is also

Received October 7, 1993; revision accepted October 14, 1993.
Address reprint requests to Richard B. Borgens, Center for Paralysis Research, School of Veterinary Medicine, Purdue University, West Lafayette, IN 47907-1244.

characteristic of most adult animal skins, including man (Kirschner, '73; Borgens, '82; Vanable, '89). A low resistance pathway to support steady polarized current flow driven by this TEP through the embryo is provided by several mechanisms: a breakdown of tight junctions in localized regions of epidermis (Decker, '81), programmed cell death producing a localized near open circuit leak such as "necrotic zones" in the limb bud (Borgens '84; Borgens et al., '87) or so-called "hind gut reduction" in the chick (Hotary and Robinson, '90), or through the interstice of the embryo continuous with the outside milieu at the blastopore (Robinson and Stump, '84). We report the existence of a steady ionic current driven out of the neural folds in amphibian embryos and confirm the blastopore current in the urodele. The neural fold currents disappear with fusion of the folds during the formation of the neural tube. These transembryo currents are associated with polarized internal electric fields of about 5–25 mV/mm.

MATERIALS AND METHODS

Axolotl embryos

Axolotl embryos (blastulae), provided by the Indiana University Axolotl Colony, were staged according to Bordzilovskaya et al. ('89). They were held in an incubation chamber at 5°C and then removed to room temperature where development continued until physiological measurements were performed on them. Prior to measurement the jelly coat and vitelline membrane were mechanically removed. During use embryos were kept at room temperature and maintained in either artificial pond water (APW) consisting of 1.5mM NaCl, 0.6 mM KCl, and 1.0 mM $CaCl_2$ or 25% Holtfreter's medium consisting of 15 mM NaCl, 0.17 mM KCl, 0.23 mM $CaCl_2$, and 0.60 mM $NaHCO_3$ (pH 7.4). The resistivity of theAPW ranged from 2,400–2,700 Ω cm and that of the 25% Holtfreter's solution from 600–650 Ω cm. Modified media used in these studies included a standard APW containing 50 μM amiloride and an APW in which recrystallized choline chloride was substituted for NaCl.

Xenopus embryos

Adult female *Xenopus laevis* (from a laboratory colony) were injected with 750–1,000 i.u. of Human Chorionic Gonadotropin to induce ovulation. Eight to twelve hours later these females were stripped of their eggs, the eggs placed in an artifically prepared culture medium, HC 1 (6.1 mM NaCl, 0.25 mM $MgCl{\cdot}6H_2O$), 0.05 mM Mg SO_4, 0.07 mM $CaCl_2{\cdot}2H_2$, 0.11 mM KCl, pH 7.0, resistivity = 1,200 Ω cm) (Robinson and Stump '84), and the supernatant from macerated testes added to the medium to fertilize the oocytes. Developing embryos were segregated into petri dishes (30–40 per dish) and stored at various temperatures (15–23°C) in order to manipulate the developmental age. Embryos were staged using the criteria of Nieuwkoop and Faber ('56). Prior to electrical measurements embryos were stripped of their jelly coat and vitelline membrane by a 10 min immersion in 2% cysteine (pH 7.8–8.0) in HC 1 followed by mechanical removal of the extraembryonic membranes. Physiological measurements began at an early stage of neural fold development (stage 15) and were discontinued at stage 33.

Vibrating electrode

The design, construction, and use of both one-dimensional and two-dimenstional vibrating probes for the noninvasive detection of extracellular ionic currents have been described (Jaffe and Nuccitelli, '74; Nuccitelli, '86; Hotary and Robinson, '92a). Briefly, the sensor in this system is a platinum tipped, parylene insulated tungsten microelectrode which is vibrated between two positions (typically a 20–200 μm excursion). Using frequency lock detection techniques, the minute voltage between the extremes of this excursion (produced by either a biological or calibration source) immersed in a conductive medium is sampled near (50–200 μm) but not touching the source. Knowing the resistivity of the medium (measured with a conductance bridge), one calibrates the system to provide the density of current entering or leaving the source using an analog of Ohm's law for extended media. This calibration was further verified by placing the vibrating electrode in an artifically imposed current of known density and direction with the plane of vibration parallel with the direction of current flow. The absence of artifactual signals (generated by a leakage of current to the medium from the voltage driven bender element of the probe) was checked for after construction or replacement of a sensor by bringing the vibrating electrode near the side of the calibration chamber or a small piece of capillary glass. The probe was vibrated at a frequency away from resonance to overcome the problem of depth-dependent changes in vibration amplitude. Permanent records were chart recordings from an Omniscribe chart recorder. In the measurements reported here, a reference line was established by moving the vibrating sensor with a micropositioner over 3 cm from the embryo and out of the electric field. The probe was then moved to one of two stan-

dard measuring positions with the center of vibration either 50 or 200 μm from the animal's surface. A deflection above the reference line indicates current entering the embryo; a deflection below the reference line indicates current leaving it. In media of the resistivity given, we routinely measured current densities on the order of tens of nanoamperes per square centimeter with a spatial resolution dependent on the sensor's size (either 35 μm or 200 μm; refer below to results). For *Ambystoma* measurements, the time constant used was 1 second and vibration frequency was about 200 Hz. For *Xenopus* measurements, the time constant used was 3 seconds and vibration frequency was 240 Hz.

For vibrating probe measurements, embryos were moved from their culture chambers to a 60 mm × 15 mm petri dish and immersed in either artificial pond water (APW) (axolotl) or HC 1 (*Xenopus*) culture medium. The bottom of the dish was covered with a 3 mm thick layer of Sylgard 184 (Dow Corning). A small pedestal was constructed of sylgard (10 mm × 4 mm) with a wedge-shaped groove that held the relatively large (approximately 2 mm) axolotl embryo in a fixed position during measurement. The density and direction of current was measured at the anterior portion of the neural folds and the lateral body ectoderm of each axolotl embryo. In *Xenopus*, stabilization of the relatively small (approximately 1.0 mm) embryo was facilitated by supporting it (dorsal surface up) with 000 insect pins inserted into the substrate. Orientation of the embryo and visual observations during physiological measurements were accomplished using a Wild stereomicroscope. A study of the variation in current density with distance from the surface allowed adjustment of all raw data to values measured at 50 μm from the surface. Surface values would be expected to be higher yet. Given the complex and varied topography, however, we chose not to extrapolate data to such uncertain values and normalized all measurements at the standard position of 50 μm for ease of comparison. Two additional axolotl embryos (stage 18) were studied with a high resolution computer assisted instrument displaying the vectoral sum of currents in two dimensions with a spatial resolution of 45 μm (Nuccitelli, '86). In studies utilizing both standard and modified APW, axolotl embryos (stage 16) were transferred through three large volumes (approximately 100 ml each) of the new test medium before being repositioned in a fourth volume where measurements were repeated. When testing the long-term effect of external Na^+ depletion on endogenous currents, embryos were maintained in large volumes of test media during the intervals between measurements.

Measurements of transepithelial potential

Measurements were made using glass microelectrodes pulled on a vertical puller (David Kopf Instruments, Model 700 C) from 1.5 mm o.d. borosilicate glass capillary tubing with an internal filament. We have used both 2 M and 100 mM NaCl filling solution, finding recorded TEPs to be equivalent. The higher molarity electrodes (with approximately 2 mV tip potentials at 30–70 meg Ωs resistance) provided more stable recordings and were used in most measurements reported here. The bath was grounded using a Ag/AgCl electrode. Electrodes were connected to a WPI Instruments Model M-707 Micro Probe System amplifier, and the measured potentials were displayed on a Fisher Recordall series 5000 chart recorder. Embryos (the jelly coat and vitelline membrane mechanically removed) were positioned (dorsal surface up) in an indentation formed for them in the 2% agar which lined the bottom of the measurement dish. Twenty-five percent Holtfreter's solution was the bathing medium used during microelectrode penetration.

RESULTS

Ionic currents during neurulation

In the axolotl (*Ambystoma mexicanum*), vibrating electrode measurements were begun at stage 15, when the neural folds were apparent. At this stage, inward and outward currents from the neural folds were detected with equal frequency. By stage 16 over 90% of the embryos (10 of 11) were driving current out of the developing neural folds. These outward currents ranged in magnitude from 0.1–1.4 $\mu A/cm^2$ (X = 0.5 μAcm^2; SEM = 0.1 $\mu A/cm^2$). With further development until stage 19, we could detect localized outwardly directed currents in 60% of the population studied (Fig. 1B). The relatively large axolotl embryos (approximately 2 mm) were scanned with the large (200 μm) sensor with the distance from the center of vibration to the embryo's surface kept at about 200 μm. The inability to detect outwardly directed currents from the comparatively small region of the folds in some embryos in these initial measurements was felt to be due to the poor spatial resolution of this large probe. Consequently, ten additional stage 17 embryos were studied with a microprobe (35 μm diameter sensor), with the center of the probe's excursion held 50 μm from the embryo's surface. In all embryos, currents were found leaving the neural folds (range = 0.3–1.0 $\mu A/cm^2$; X = 0.6 $\mu A/cm^2$; SEM = 0.1 μA/

cm^2). Outward currents disappeared completely from the area of cranial enlargement subsequent to neural tube formation. Only inwardly directed currents could be detected in this region (18 of 18 embryos, stage 20.5–21: range = 0.5–4.4 $\mu A/cm^2$, X = 1.2 $\mu A/cm^2$, SEM = 0.2 $\mu A/cm^2$). Both embryos studied with a two-dimensional probe possessed currents (approximately 1 $\mu A/cm^2$) leaving the walls of the neural folds at stage 18 (Fig. 2). Current densities averaging about 1.2 $\mu A/cm^2$ (stage 15–21) were measured entering the general body surface of all embryos (excluding the neural folds and blastopore). Both left and right sides of *Ambystoma* embryos were analyzed. The loops of outward current at the neural folds were bilaterally symmetrical, with current returning through the neural plate and body surface. In axolotl embryos we noticed a leveling of these magnitudes of current leaving the neural folds. In contrast, ionic currents entering body epidermis increased in magnitude after stage 15 (Fig. 3).

Currents similar to those leaving the lateral walls of the neural folds in salamander embryos were also detected in frog embryos (*Xenopus laevis*). Measurements were begun at stage 15, at which time the neural folds were already apparent in *Xenopus* embryos. From this stage until just prior to the closure of the neural folds to form the neural tube (stages 18–19), the dorsal and cranial region of 16 embryos was characterized by currents (range = 1.0–6.9 $\mu A/cm^2$; X = 3.2 $\mu A/cm^2$; SEM = 0.5 $\mu A/cm^2$) leaving the lateral walls of the neural folds (Figs. 1A, 4A). When the probe was moved from a position adjacent the lateral wall of the neural fold, across the shallow groove where the neural folds merge into the swelling of the embryo's body wall, the large currents leaving the neural fold were observed to decrease in magnitude and finally reverse their polarity when the vibrating electrode was positioned over the flank proper. In six of these embryos, measurements were made well into stages 18–21 (where the neural folds begin to fuse dorsally to form the neural tube). In five of these, currents leaving the lateral wall of the neural fold disappeared (Fig. 4B). In the sixth embryo, a small patch (about 0.3 mm^2) of outward current was still observed directly dorsal to the eye primordium at the most anterior margin of the cranial enlargement. After the neural tube was well formed (stage 21–25), the 18 embryos scanned were characterized by weak currents entering the dorsal regions of the neural tube and the developing cranial enlargement (range = 0.4–2.6 $\mu A/cm^2$; X = 1.4 $\mu A/cm^2$; SEM = 0.7 $\mu A/cm^2$) (Fig. 4B–D).

Later stages of development were studied in 43 additional *Xenopus* embryos, with emphasis on the regions of optic and otic primordia (Fig. 4B–D). Of the 40 individuals in which the optic primordium was scanned, in only three were outwardly directed currents (0.1–0.4 $\mu A/cm^2$) observed. In 17 embryos, the otic placode was scanned between stages 21 and 33. Currents were detected entering the placode in 11 of these (0.1–4.7 $\mu A/cm^2$; X = 0.9 $\mu A/cm^2$; SEM = 0.3 $\mu A/cm^2$). In the other six, measurements were confounded by shifting polarities of current entering or leaving the nearby brachial region. Such transitory shifts in ionic current at the developing brachial arch, and in later stages the more well-developed gill, were not uncommon. These rapidly shifting and variable currents might be expected in this area, were noted, but not examined further. These regions were not examined in axolotl embryos. We made no attempt to systematically study the caudal-most neural fold in either species. The much greater density of current leaving the blastopore dominates recordings made with the sensor up to 200 μm from the surface.

Fig. 1. Ionic current traversing amphibian neurulae. **A:** Neurulation currents in *Xenopus laevis*. To the left, vibrating electrode record of a scan of the developing neural folds at stage 16/17. To the right, an illustration of the measurement positions. A reference line (R) was established by moving the probe more than 3 cm from the embryo and out of the electrical field. The probe was then moved to a standard measurement position 50 μm from the embryo's surface. A deflection above the reference line indicates current entering the embryo; a deflection below the reference line indicates current leaving it. Measurement began in the mid-flank region (a,b) moving dorsal adjacent to the neural folds and rostral (c,d,e); then ventral, crossing to the flank (f,g,h); rostral, and then dorsal to the neural fold (i-m); then to the anterior flank (n,o). The sensor's tip size was 35 μm, vibration distance approximately 30 μm, and embryo diameter approximately 1 mm. Note the shifting polarity of current throughout the scan: current emerging at the folds; falling to baseline levels at the boundary of fold and flank ectoderm; and reversing to inward over regions of flank ectoderm. **B:** Neurulation currents in *Ambystoma mexicanum*. To the left, vibrating electrode record of a scan of developing neural folds at stage 17/18. To the right, an illustration of the measurement positions. Reference line (R) and current conventions as above. The probe was then moved to a standard measuring position with the center of vibration 200 μm from the animal's surface. The plane of the probe's vibration was held perpendicular to the wall of the neural folds (plane 2) or slightly oblique (dorsalateral) (plane 1). The outward currents detected at position a and b presented in this record were made at plane 1. The inward current recorded over body epidermis (C) was typical of ionic currents entering the rest of the embryo. The probe tip was 200 μm and neurulae approximately 2 mm in length.

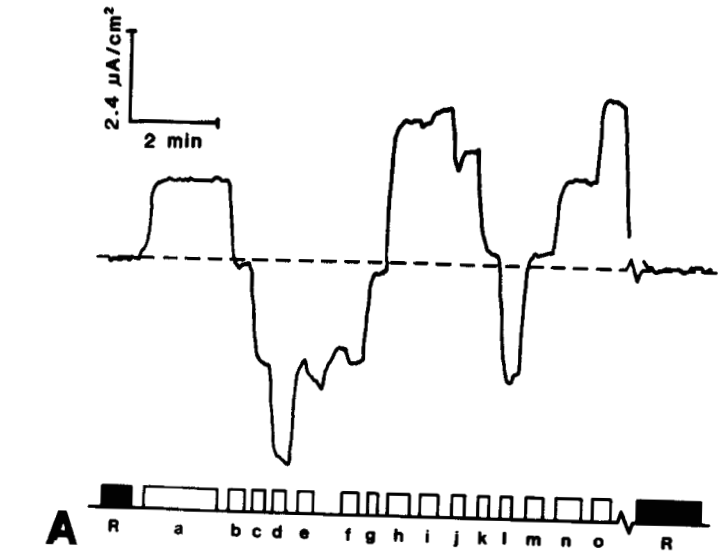
2.4 µA/cm²
2 min
A
R a b c d e f g h i j k l m n o R

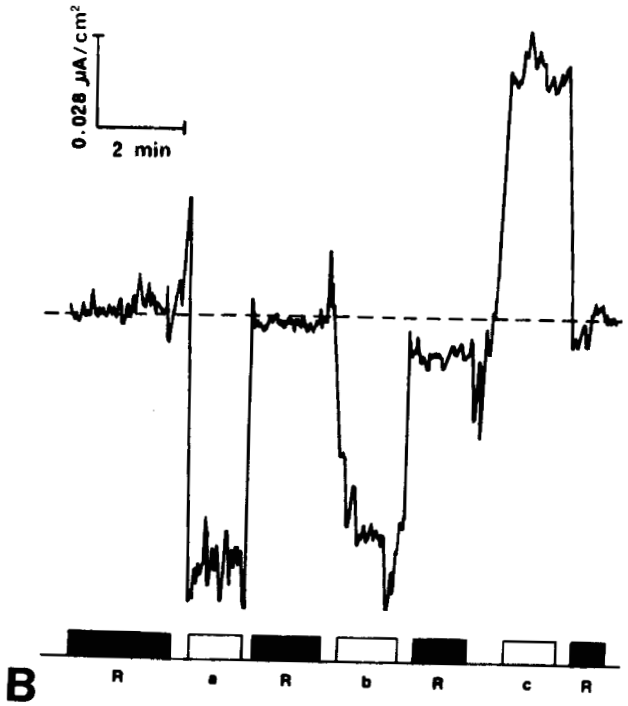
0.028 µA/cm²
2 min
B
R a R b R c R

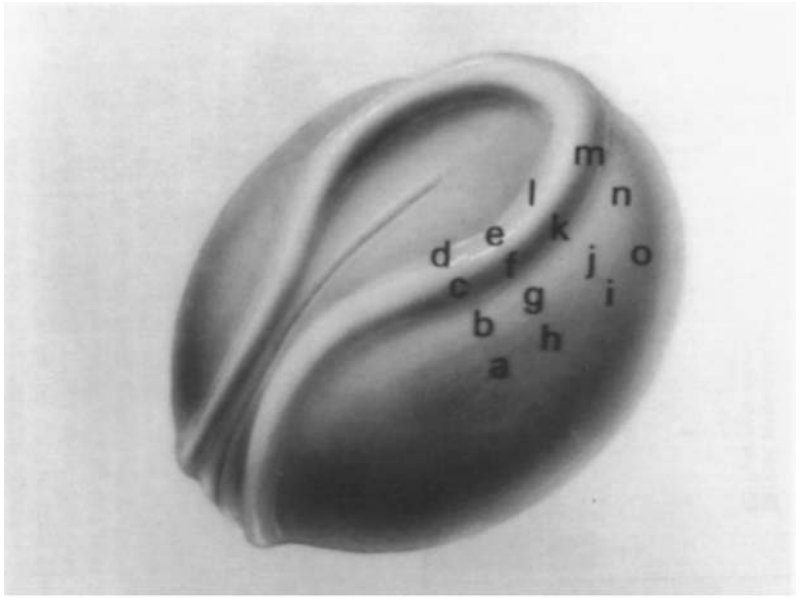
m
l
n
k
d
e
j
o
f
i
g
b
h
a

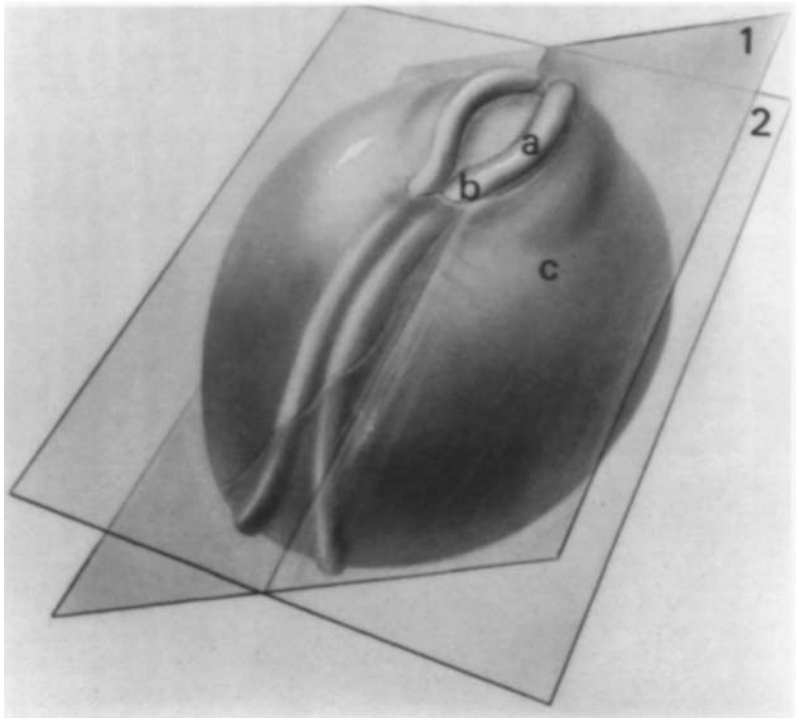
1
2
a
b
c

Figure 1.

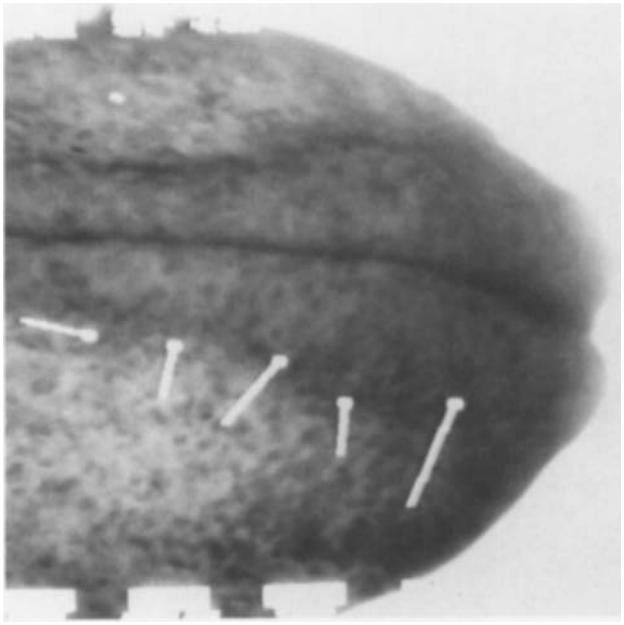

Fig. 2. Neural fold currents in an Axolotl embryo (stage 18) detected with a two-dimensional vibrating electrode. The 30 μm diameter sensor was moved in a circular excursion in a plane horizontal to, and 50 μm from, the embryo's surface. Both orthogonal components of an ionic current were measured simultaneously and represented as a current vector, superimposed on the video image of the neurula. Current vectors are displayed as a line originating at a dot which marks the measurement position. The direction of the line from the dot denotes the direction of current flow, and the length of the line is proportional to its magnitude (1 cm = 1μA/cm^2). Note the outwardly directed currents at the edge of the cranial neural folds.

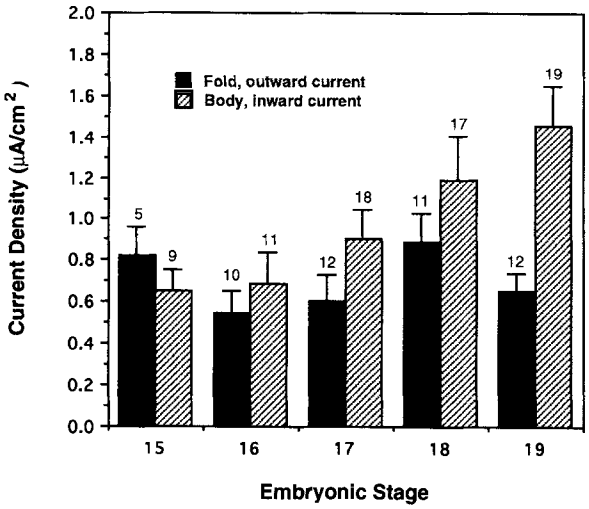

Fig. 3. Ionic currents entering or leaving axolotl embryos as a function of stage. The currents entering the body epidermis (hatched bars) increase steadily in magnitude with development. The mean current densities at stages 19 and 15 are significantly different ($0.01 < P < 0.02$ Mann Whitney and Student's t-test). The number of embryos measured at each stage is depicted above the error bars. Currents leaving the folds in this population (solid bars) did not vary greatly in magnitude, and the difference between groups is not significant. Only stages prior to neural fold closure are depicted. Though solid bars are all outwardly directed current and hatched bars inwardly directed, they are plotted side by side to facilitate comparison of their magnitudes.

Measurements of transepithelial potential

Internally positive transepithelial potentials ranging from 18–64 mV were immediately and easily recorded following impalement of the ectoderm. We first examined the distribution of the transepithelial potential at 12 loci in each of four stage 16 axolotl embryos (Fig. 5). The distance between the measurement positions along the length of the embryo was approximately 400 μm. The order in which these loci were examined was randomly selected for each embryo. Internally positive potentials were seen at each recording site in all 4 embryos. An analysis of the magnitude of TEP recorded at these various locations revealed a caudally negative voltage gradient under the neural plate in each of the four embryos examined, though variation in the magnitude of the TEPs between embryos was observed. This gradient was 5, 7, 20, and 23 mV/mm in the four neurulae, respectively, across the length of the body axis (under the neural plate) (Fig. 6). The recorded gradient between any two measurement positions was often considerably higher, up to 63 mV/mm. The mean potential at the anterior-most recording site of the neural plate was 54 mV (SEM = 4 mV), while that at the posterior-most site was 39 mV (SEM = 7 mV). The difference in the TEP between these sites is significantly different ($0.02 < P < 0.05$, one-tailed Student's t-test).

This gradient was further explored in eight additional stage 16 embryos. In this second series of measurements, seven locations along the longitudinal axis of the neural plate were sampled. The most rostral was at the junction of fold and neural plate; the most caudal was approximately 50 μm from the blastopore. As in the previous measurements, all TEPs recorded were internally positive, and a consistent caudally negative profile was observed. This rostral/caudal potential gradient of 10 mV/mm (range 1–24 mV/mm; SEM = 2.54 mV/mm) (Fig. 7). Statistical comparison between pooled data taken at positions 1 and 7, 2 and 6, and 3 and 5 were significant ($P < 0.005$, $P < 0.005$, and $P < 0.05$, respectively (Fig. 7). TEPs were consistently

higher in the rostral lateral flank ectoderm (X = 45 mV; SEM = 7 mV) than in the caudal flank (X = 40 mV; SEM = 5 mV) in each of the first four embryos studied. These differences were not statistically significant given the variations in data and the few embryos studied.

Na^+ dependence of the neurulation currents

When Na+ was replaced with choline or increased over threefold in the measurement medium, ionic currents leaving the axolotl's neural folds were eliminated (n = 4), or doubled in magnitude (n = 6), respectively (Fig. 8). Exchanging the measurement medium with one containing 50 μM amiloride (a potent Na^+ channel blocking agent [Borgens et al., '77, '79b; Sariban-Sohraby and Benos, '86]) immediately eliminated outwardly directed currents in two embryos and reduced outward currents at the folds to less than 40% of their initial magnitude in a third embryo but did not affect the ionic currents in a fourth. Identical responses to Na^+ modulation were observed in the same embryos when testing inwardly directed flank currents. The effect of amiloride on blastopore currents was also tested in three *Xenopus* embryos. Four separate measurements were made to establish the peak density leaving this region for each embryo (8.3, 3.6, and 16.8 $\mu A/cm^2$). After a 15 min immersion in HC 1 containing 10 μM amiloride, an identical series of measurements was repeated for each individual. Peak currents recorded were reduced to 0.7, 0 (no current detected), and 3.2 $\mu A/cm^2$, respectively.

The effect of prolonged Na^+ deprivation on ionic currents was examined in an additional seven embryos. Currents entering or leaving the flank and blastopore of stage 16 axolotl embryos were first measured in standard APW. Each embryo was then transferred to the new test medium and measurements were repeated periodically for up to 8 h (Fig. 9). When placed in choline APW (n = 3), the inward currents at the flank were eliminated or reduced by about 75%, while the outward currents at the blastopore fell by more than 90% of their original magnitude (Figs. 8, 9). The magnitude of the inward flank current had returned to normal within 2 h in one embryo and within 4 h in the remaining embryos. The outward currents at the blastopore returned in similar fashion, though in one embryo the current never regained its original density. When placed in APW containing 50 μM amiloride (n = 4), a reduction by 50–90% and 75–98% of the original magnitude was observed in the inward flank and the outward blastopore currents, respectively (Fig. 10). Within 2 h currents at both surfaces had normalized in a single embryo and within 4 h in a second. In the third embryo the inward flank current, but not the blastopore current, reached its original magnitude within 4 h and that of the fourth embryo within 6 h.

In an effort to determine if this transitory (2–4 h) interruption of natural currents (and therefore an interruption in the internal voltage gradients) results in abnormal patterning, axolotl embryos were cultured in either 50 μM amiloride APW (n = 15) or choline substituted APW (n = 15) throughout the period of neurulation (beginning at stage 13.5). All embryos were then transferred to standard APW at stage 21/22 when fusion of the neural folds was completed and reared to stage 36–39, at which time they were sacrificed for histology. All embryos in the amiloride group, as well as an approximately equal number of control embryos (reared solely in APW), displayed normal morphology. Though 2 of the 15 embryos cultured in choline substitued APW possessed abnormalities (blisters in head and hindbrain regions in one and enlarged abdomen in the other), this result is not statistically significant ($P > 0.05$, chi-square test).

DISCUSSION

Prior to closure of the neural folds, a steady ionic current is driven out of both lateral walls of the folds and the blastopore in both *Xenopus laevis* and *Ambystoma mexicanum*. These outwardly directed currents disappear in both species coincident with the fusion of the neural folds. The blastopore current can still be detected following neural tube formation in the anuran and urodele (Robinson and Stump, '84; Borgens, unpublished observations). In *Xenopus* we detected little change in the polarity or magnitude of ionic current coincident with the formation of the optic vesicle and otic placode or their differentiation during later stages of development. In both species, focused outwardly directed current localizes the pre-limb bud region of flank ectoderm in more mature larvae (Borgens et al., '83; Robinson, '83; see below).

All of these transembryo currents are driven by the internally positive TEP of the ectoderm and would be associated with an internal voltage gradient increasingly negative at the subepidermal region where current emerges from the embryo or larvae. We provide measurements of one of these internal electric fields organized in the rostral/caudal plane beneath the neural plate in stage 16 axolotls (Fig. 11). This gradient is on the order of 10 mV/mm and was distally negative in each of

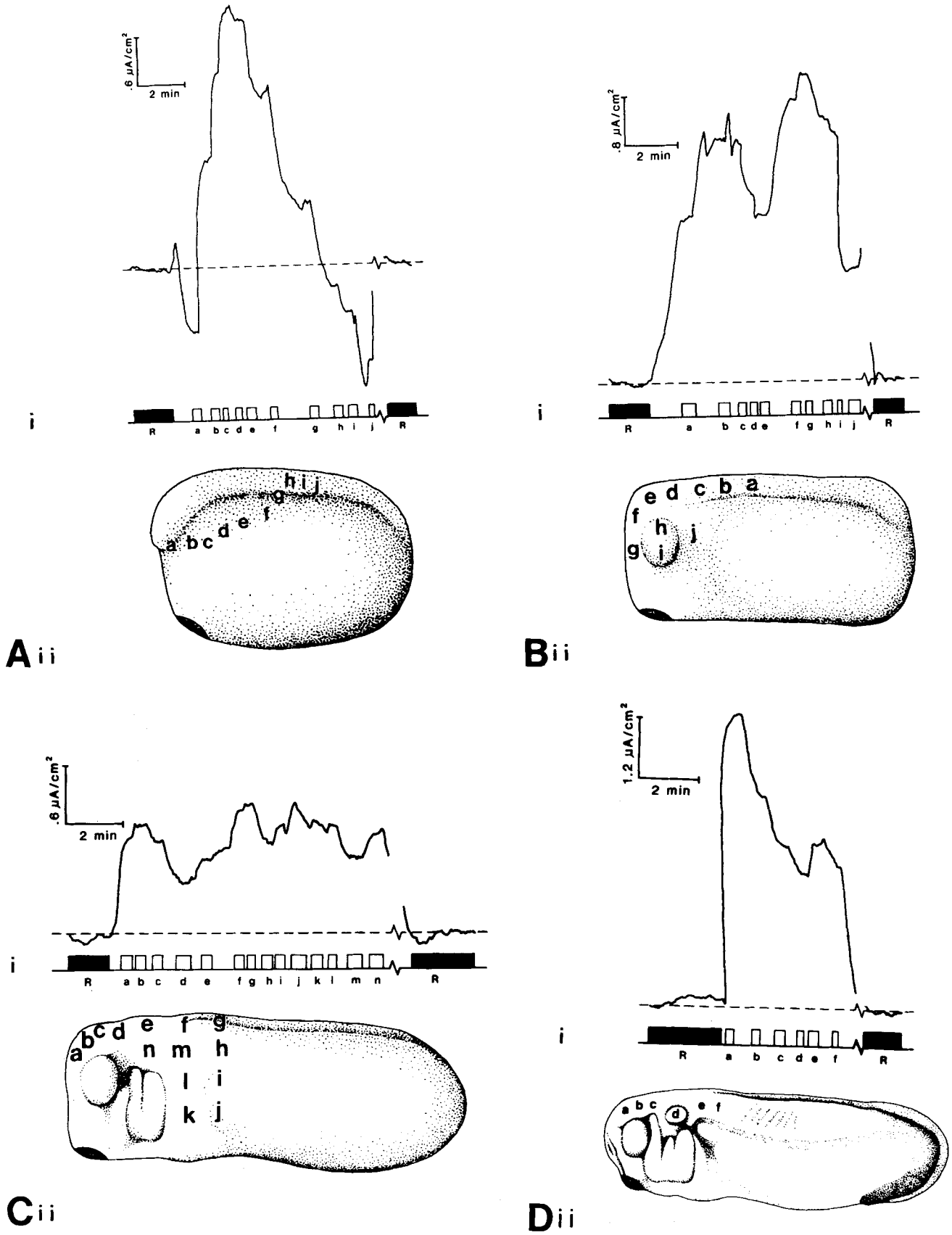
.6 µA/cm²
2 min
i
R a b c d e f g h i j R
a b c d e f g h i j
Aii
.8 µA/cm²
2 min
i
R a b c d e f g h i j R
a b c d e f g h i j
Bii
.6 µA/cm²
2 min
i
R a b c d e f g h i j k l m n R
a b c d e f g h i j k l m n
Cii
1.2 µA/cm²
2 min
i
R a b c d e f R
a b c d e f
Dii

Figure 4.

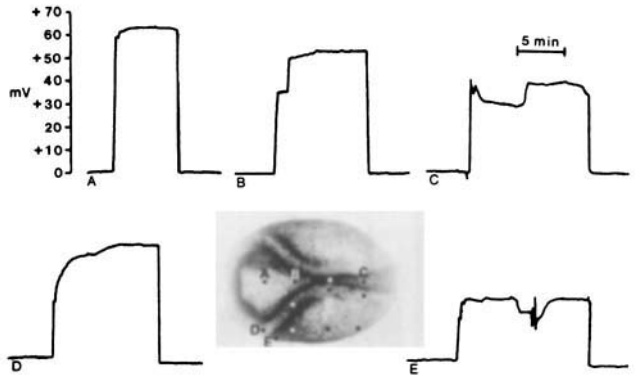

Fig. 5. Measurements of TEP in an axolotl neurula. The insert shows the 12 standard measurement positions, approximately 400 μm apart in the rostral/caudal axis along the neural plate, in the neural fold, and flank ectoderm. Records (**A–E**) are presented for 5 of these 12 positions. The abrupt shift (upward) in each record indicates the shift in potential at the moment of microelectrode impalement of the ectoderm. Inwardly positive potentials were relative stable for 5–15 min of recording, and all records were taken with the same microelectrode. Note the approximate 40–50% fall in the magnitude of recorded TEP from that observed at the rostral neural plate as more caudal or more lateral regions of ectoderm were sampled. This would be associated with an increasingly more negative gradient of subectodermal potential at caudal or more lateral regions relative to the cranial neural plate.

the 12 embryos studied. Such internal voltages are within a range known to affect the shape and the migration of embryonic cells in vitro (reviewed by Robinson, '85, Nuccitelli, '88, Borgens, '92).

Our continuing studies demonstrate that 1) the TEP of the lateral margin of the neural fold is consistently negative with respect to adjacent ectoderm in the transverse axis; 2) the rostral/caudal gradient beneath the neural plate begins to become apparent at stage 15 and disappears by stage 18/19 in axolotl neurulae; and 3) the appearance/disappearance of the rostral/caudal gradient relates more to the presence of the neural fold currents than the blastopore current (Shi and Borgens, unpublished observations). These data will be the subject of the third paper in this series.

It is now quite clear that ectodermal "batteries" drive polarized current through a wide variety of embryos, including the frog, salamander, chick, and mouse (see below). The magnitude of the internal fields have only been described in one other of these models. Approximately 20 mV/mm fields are associated with posterior intestinal portal current densities on the order of 100 $\mu A/cm^2$ in the chick (Hotary and Robinson, '90). We report a similar potential drop along the longitudinal axis of the axolotl beneath the neural plate associated with externally detected current densities only a fraction of those measured in the chick. Hotary and Robinson ('90:157) suggest "the size of the current is relevant because it will directly determine the size of the internal voltage gradient." This is an oversimplification. The magnitude of voltage gradients associated with extracellular currents in animals and plants is more related to the cross-

Fig. 4. Ionic currents traversing CNS specialization in *Xenopus* embryos and larvae. **A:** One-dimensional vibrating probe scan of region of prospective optic primordium and neural folds in a stage 17/18 embryo (Nieuwkoop and Faber, '56). **i:** Vibrating electrode record. Reference and other conventions as in Fig. 1. Probe and measurement parameters as in Fig. 1A. **ii:** Illustration of the measurement positions depicted above. Note the presence of outwardly directed current at the margin of the anterior neural folds (a) and the reversal of polarity as the probe scans the surface over regions of subsequent eye development (b–g). The polarity of current reverses again at the neural folds, position h–j. (The break in the record represents 3 min of recordings made elsewhere). **B:** Ionic currents traversing the optic primordium and neural tube. **i:** Vibrating probe record of scans in a stage 19–20 embryo. **ii:** Illustration of the measurement positions depicted above. This probe record begins with measurements of current entering the lateral wall of the neural tube (now closed) (a), proceeding cranially to the most anterior margin of the cranial enlargement (b–g). Measurements were taken directly adjacent to the eye vesicle (h,i), and further measurements were made just caudal to the eye vesicle (j). Note the absence of outwardly directed currents in any of these regions. The break in the record represents 2 min of recording time where other regions of the embryo were explored. **C:** Ionic currents entering the epidermis of the lateral wall of the neural tube and regions of presumptive otic placode formation. **i:** Vibrating probe records of a scan made in a stage 22 embryo. **ii:** Illustration of the measurement positions depicted above. This scan begins with measurements made adjacent to the epidermis of the cranial enlargement (a), moving caudally along the well-formed neural tube (b–g). The measurements were shifted ventrally, along the body wall (h–l) with a focus on the region of presumptive otic placode formation (m–n). Note the presence of current entering all of these regions. The break in the record represents 12 min of measurement where other regions of the embryo were explored. **D:** Ionic currents traversing the more differentiated nervous system including the epidermis of the otic vesicle. **i:** Vibrating probe records of a scan made in a stage 29 embryo. **ii:** Illustration of measurement positions depicted above. This scan begins adjacent to the anterior and lateral wall of the cranial enlargement and moves caudally along the dorsolateral region of the embryo, including a measurement directly adjacent the otic vesicle (position d). Note the presence of inward currents in these regions. The break in the record indicates 2.2 min of recording time where other regions of the embryo were explored. A 35 μm diameter probe was used in these measurements, keeping the center of the probe's excursion approximately 50 μm from the embryo's surface. The illustrations are not drawn to scale; neurulae (as in A,B) » 1.0–1.5 mm in length; as in D, 2.7–3 mm in length.

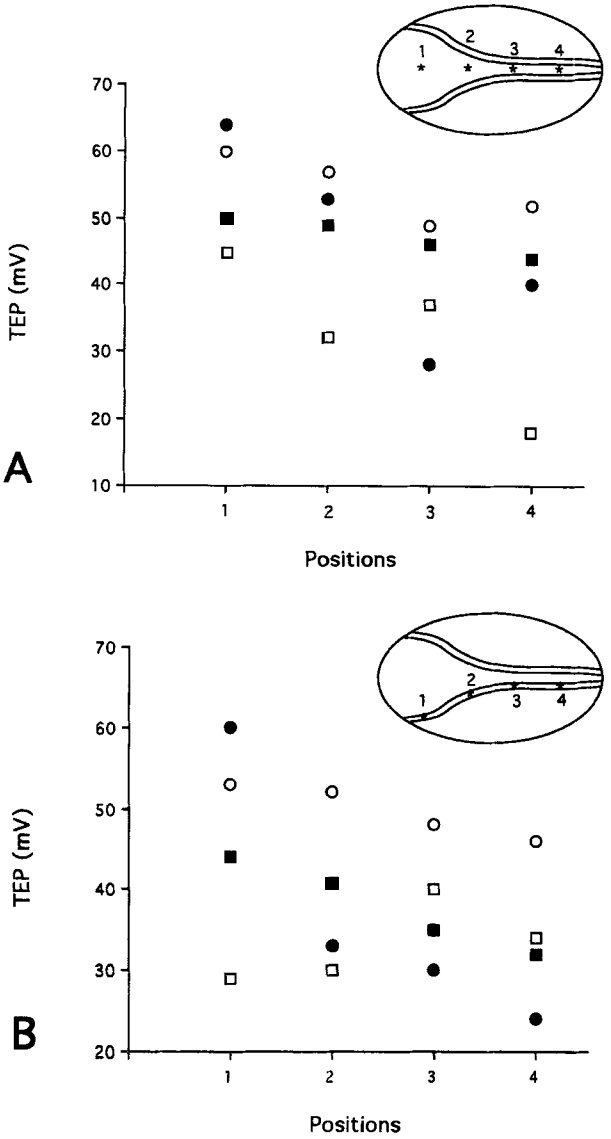

Fig. 6. Distribution of the neural plate and neural fold TEP in stage 16 axolotl neurulae. The magnitude of the TEP recorded from four locations approximately 400 μm apart along the length of the neural plate (**A**) and neural fold (**B**). Position 1 refers to the rostral-most recording site; position 4 refers to the caudal-most recording site of each region (as depicted by stars in insets; see also inset, Fig. 5). Individual sets of data for four separate neurulae (○, ●, □, ■) are displayed.

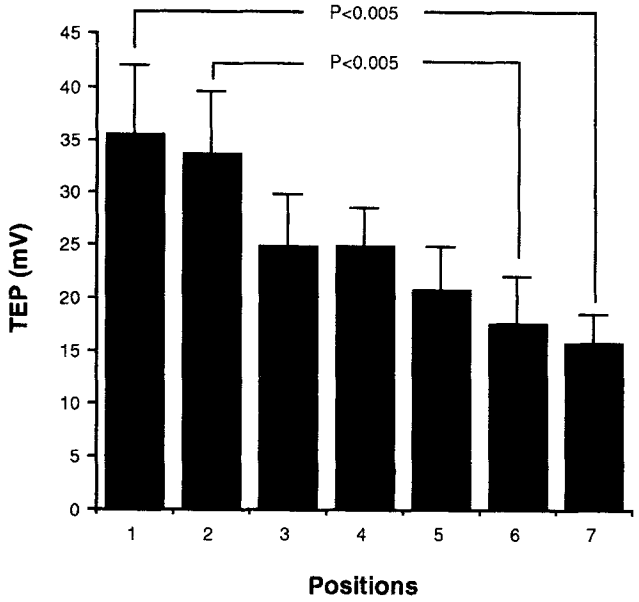

Fig. 7. Rostral/caudal voltages beneath the neural plate in stage 16 axolotls. The magnitude of the neural plate TEP in eight embryos sampled at seven positions in the longitudinal axis is presented. Position 1 was at the most rostral margin of plate and fold, while Position 7 was the most caudal, approximatley 50 μm from the blastopore (statistical evaluation; Student's *t*, one-tailed). Note the marked caudally negative slope in electrical potential.

sectional area of the extracellular space between cells (Jaffe '79, Borgens, '82), and the two are inversely proportional. Relatively weak densities of extracellular current can produce relatively steep extracellular electric fields when current is constrained to flow through tissue regions where the cross-sectional area of the extracellular space is limited (Jaffe, '79; Borgens, '82). Attempts have been made to analyze the slope of the voltage profiles within animals by so-called "cable analysis." Extracellular voltages associated with injury currents in mammalian skin wounds appeared to provide only fair to good fit following cable evaluation (Table 3 in Barker et al., '82), and do not fit at all in studies of limb stump currents and voltages in salamanders (McGinnis and Vanable, '86). An exponential increase in the slope of internal voltages (suggested by cable analysis) nearer to a focused current leak was not observed in measurements of chick posterior intestinal portal currents nor in the sub-neural plate voltages described here. These physiological measurements raise a cautionary note when applying theoretical evaluation of electrical parameters when the exact pathway of internal currents and the relevant cellular geometries along this pathway are unknown.

Endogenous currents in developing vertebrates

In the amphibian embryo, steady current has been detected leaving the region adjacent to the first cleavage and subsequently each blastomere drives a current through itself—current leaving the basolateral domain (Kline et al., '83). Steady ionic

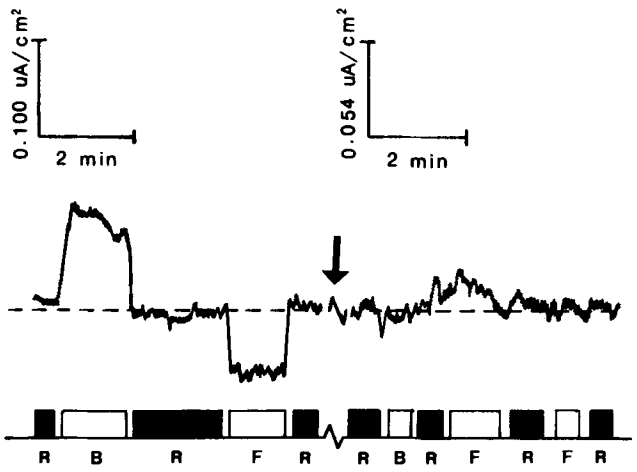

Fig. 8. Na^+ dependence of axolotl neurulation currents (reference and current conventions as in Fig. 1). Steady current (0.05 $\mu A/cm^2$) was detected entering the body epidermis adjacent to the neural folds as well as leaving the neural folds of this stage 16 embryo. The APW (Na^+ = 1.5 mM) was exchanged with 5 mM Na^+ APW (record begins here). Note the roughly twofold increase in current density entering the body epidermis (B) and leaving the neural folds (F) in the presence of 5 mM Na^+. This high Na^+ APW was subsequently (break in the record at arrow) replaced with a medium in which recrystallized choline was substituted for the Na^+. After 5 min, currents entering the body (B) were no longer detected, and currents leaving the folds (F) had fallen to baseline or slightly reversed their polarity. The change in scale reflects the differing resistivities of 5 mM Na^+ APW (1,350 Ω cm) and choline chloride APW (2,500 Ω cm).

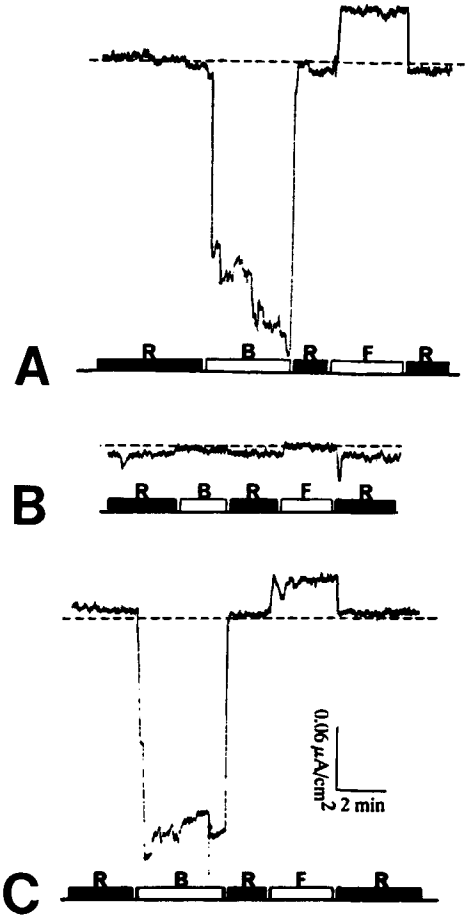

Fig. 9. Vibrating probe record of the adaptation of flank and blastopore currents to Na^+ depleted media. **A:** Currents leaving the blastopore (B) and entering the flank (F) in normal artificial pond water (APW), B: Same measurements after 10 min immersion in a choline-substituted APW (see Materials and Methods), **C:** Same measurements after 2 h in the same medium shown in B. R = reference line (hatched line) where the probe was more than 3 cm from the embryo and out of the electric field. The probe was then moved to a measurement position 150 μm from the embryo's surface for measurements at B and F. Note the elimination of both flank and blastopore current in **B** and their return to near normal values by 2 h (C). Scale in C is the same for all three sets of measurements, as the resistivity of APW and choline APW is the same.

current has also been measured leaving the basal domain of mouse blastomeres and leaving the primitive streak of chick and mouse embryos (Jaffe and Stern, '79; Nuccitelli, '88; Winkel and Nuccitelli, '89). These transembryo currents have been suggested to play a role in the establishment of polarity in embryonic epithelium, but this has not been directly tested. During later development of the chick embryo, a large leakage current (approximately 100 $\mu A/cm^2$) has been detected leaving the posterior intestinal portal (Hotary and Robinson, '90), producing an internal potential gradient of about 20 mV/mm in the caudal region of the embryo. When this leakage current was reduced by about 30% using implanted current shunts, abnormalities in tail development and in other regions of the embryo resulted (Hotary and Robinson, '92b). This direct test suggests the intestinal portal leak is indeed relevant to tail morphogenesis in the chick.

The endogenous currents reported here in anuran and urodele embryos both confirm and correct a prior report by Robinson and Stump ('84). These investigators noted outward currents at the blastopore in *Xenopus* embryos but reported inwardly directed current at all other regions, including the neural plate. Had they positioned their probe normal to the lateral walls of the neural folds, they might have observed the outwardly directed current described here. We note as well some incidence of transitory outwardly directed current that is not due to mechanical damage around the brachial area, and in rare instances we have detected weak outward currents over the developing optic and otic

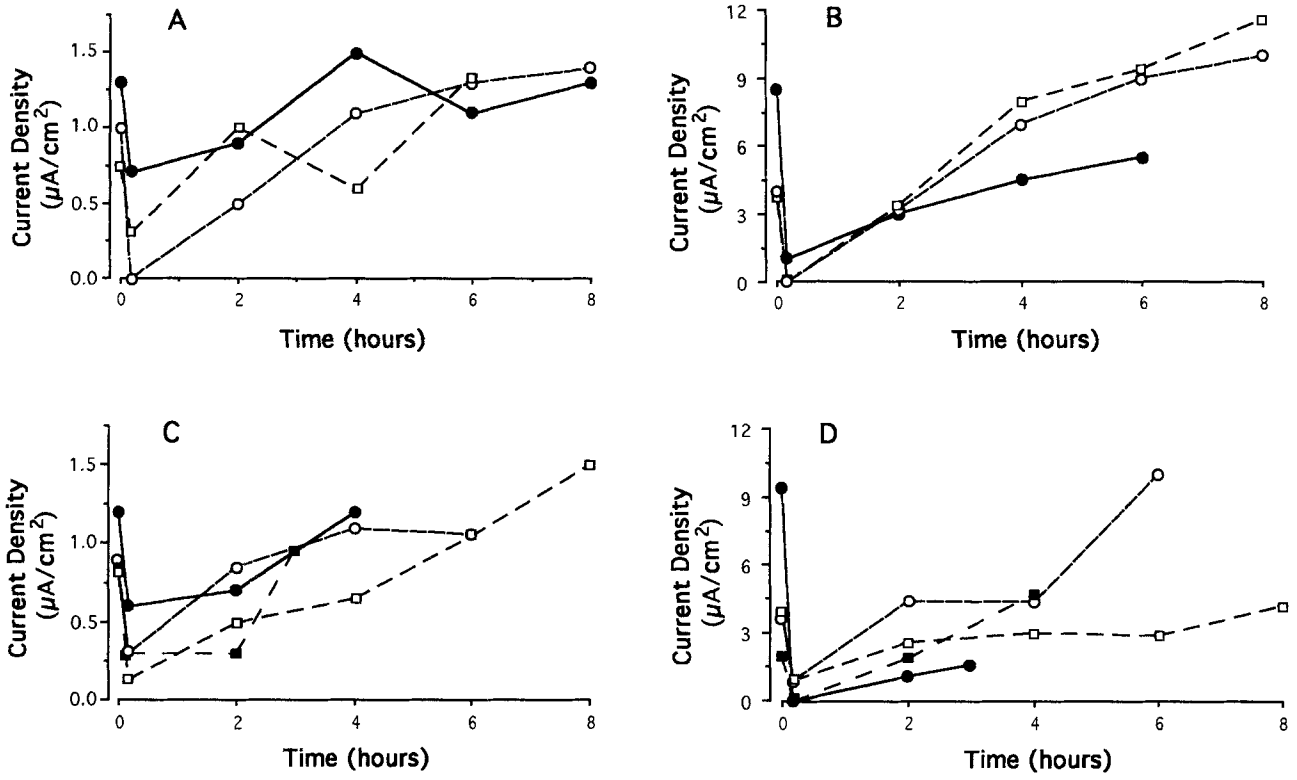

Fig. 10. Effect of chronic immersion in choline-substituted artificial pond water and Amiloride on the magnitude of ionic currents. **A:** The effect of Na^+ depleted (choline-substituted) media on ionic currents entering ectoderm is shown measured with a vibrating electrode at the midlateral flank. Three individual sets of data for separate neurulae (●, ○, □) are displayed. Note the reduction in the density of current following medium substitution (time 0). **B:** A similar set of data for the same three neurulae is displayed; however, ionic currents leaving the blastopore were analyzed. Note the marked (50% or greater) reduction in the density of current after substitution of APW (time 0) for Na^+ depleted media. At both flank and blastopore a graded return to near normal values was observed by at least 2 h. The effect of chronic immersion in 50 μM Amiloride-treated APW on ionic currents entering the flank (**C**) and ionic currents leaving the blastopore (**D**) are shown. A set of data measured in four individual neurulae (●, ○, ■, □) are displayed. The density of ionic current in normal APW is shown at time 0, followed by a substitution of this medium with APW containing 50 μM amiloride. Note the marked reduction (50% or greater) within 10 min following amiloride treatment. A graded recovery to near normal values was observed in about 4 h in all but one embryo.

regions. These do not, however, detract from the general rule that inwardly directed steady ionic current (on the order of a 1–2 $\mu A/cm^2$) enters most of the surface of the early developing amphibian and leaves the neural folds and blastopore.

In later larval development in both *Xenopus laevis* and *Ambystoma mexicanum*, an outwardly directed current accurately predicts the region of limb bud emergence (Borgens et al., '83; Robinson, '83). Though spatially focused and developmentally prophetic, the relevance of this current to limb primogenesis has not been directly tested. The relevance of endogenous current to limb development receives support from direct tests of a similar outwardly directed current (approximately 100 $\mu A/cm^2$; 60 mV/mm) accompanying forelimb regeneration in adult urodeles (reviewed by Borgens, '89).

The ectodermal battery

We provide evidence that the ionic currents traversing the amphibian embryo are produced by the TEP of the embryonic ectoderm. This inwardly positive voltage, expressed across the integument, has been well characterized in adult amphibians and other vertebrates (reviewed by Borgens '89, Vanable, '89) and has been reported in *Xenopus* embryos (McCaig and Robinson, '82) and observed in gastrulating axolotls and their neurulae (see Metcalf and Borgens, this issue). In embryonic and adult amphibians the magnitude of the TEP is usually immediately and reversibly responsive to

Fig. 11. Videographic illustration of stage 16 axolotl embryos demonstrating TEP distribution. The false color scale at the left displays the TEP measured by microelectrode impalement of neural plate, neural fold, and flank ectoderm taken from data presented in Figs. 5–7. The first embryo shows rostral/caudal gradients in TEP in neural fold and neural plate. The two additional embryos show a similar distribution of TEP in the neural plate. These three examples demonstrate the range of potentials observed in all 12 embryos.

changes in the concentration of Na^+ in the incubation medium or to blockage of Na^+ channels at the outer layers of the epidermis with amiloride, benzamil, the methyl ester of lysine, and other agents dilute in the bathing medium (reviewed by Borgens, '89; Sariban-Sohraby and Benos, '86). The acute reduction (or elevation) of current traversing the embryo by Na^+ modulation is strong evidence for its generation by the TEP.

We, as well as others, have referred to the TEP of the amphibian integument as "Na^+ dependent"; however, this is something of an overstatement. Short circuit current driven by the TEP is reduced or eliminated by reducing or eliminating Na^+ flux across the skin, but only temporarily. We have reported "adaption currents" in adult urodeles in response to a chronic reduction in TEP by modulating Na^+ uptake (Borgens et al., '79b) and have reported here a similar reappearance of ionic current traversing axolotl embryos and larvae cultured in Na^+ depleted media or media containing 50 μM amiloride. The ionic dependence of such adaption currents is unknown. It is also unknown if increased levels of current and voltage generated by the skin in response to elevated Na^+ will fall to more nominal values, modulated by the skin's intrinsic abilities to regulate its TEP by regulating the ionic fluxes across itself.

Amphibians develop normally in fresh waters of a wide range of ionic strengths and Na^+ concentrations. Here we have used several culture media commonly employed in the laboratory ranging from 1.5 mM (APW) to 15 mM external Na^+ (25% Holtfreter's solution). These media were chosen to provide the best viability for embryos and for those following removal of the vitteline membrane (see Armstrong et al., '89, Robinson and Stump, '84). While externally detected current densities in *Xenopus* neurulae (using HC 1; 6 mM Na^+) at first glance appear generally higher than similar currents in axolotl (measured in APW), this is probably due to the higher molarity of Na^+ in the *Xenopus* bathing medium. It is unlikely that this is a characteristic difference between species; similar current densities would probably be observed if both were measured in the same medium, though variation between individual embryos was observed in each species. Moreover, while the measurements of TEP in axolotl revealed gradients of potential in any one individual neurula, the magnitude of TEPs between individuals varied considerably as well.

The migratory and conformational responses of single cells may vary critically over a modest range of externally applied fields in the physiological range (1–50 mV/mm) (Robinson, '85; Nuccitelli, '88; Nuccitelli and Erickson, '83). It follows then, that development, if dependent on similar endogenous voltages, might be clearly retarded or accelerated depending on the salinity of the culture media, the

resultant magnitude of the TEP, and finally transembryo currents and potential gradients generated by the TEP. Given the individual variation noted above and unknown homeostatic physiologies of the embryonic ectoderm, any relationship between development and the salinity of external media would only be weak evidence for or against the critical nature of endogenous currents and electric fields to ontogeny. What would be more relevant are direct tests of this hypothesized relationship such as the correlation of defective tail development in the chick embryo with a chronic reduction in ionic current leaving the posterior intestinal portal. This reduction was accomplished through the use of hollow "shunts" that when inserted through tail ectoderm provided a secondary low resistance current leak that reduced the net current driven out the intestinal portal (Hotary and Robinson, '92b). The large, well-developed, and sturdy chick embryo (stage 11–15) permits the use of such shunts. The more delicate neurula stage urodele embryo is more easily damaged, and we have not overcome technical difficulties associated with the use of similar shunts in developing amphibians. We have made a preliminary test of the relevance of the trans-embryo currents and fields by maintaining neurulae in Na^+ depleted media or in culture media containing amiloride. Both treatments were designed to reduce or eliminate endogenous fields. These manipulations failed to interfere with development but also failed to reduce the ionic currents for any substantive period. Other tests, however (see below), do support the critical nature of the currents and voltages described here.

Voltage gradients and molecular determinants of pattern

We imagine that endogenous DC fields may act in concert with other known determinants of vertebrate pattern in at least three ways: 1) Extracellular voltages can produce asymmetries in the distribution of various cell surface receptor molecules including ACh (Luther and Peng, '85) and lectin (Poo and Robinson, '77) receptors in muscle, lectin receptors in macrophages (Orida and Feldman, '82) and neuroblastoma (Zagyansky and Jard, '79), EGF receptors in A431 cells (Giugni et al., '87), and lipoprotein receptors in fibroblasts (Tank et al., '85). If the topological features of receptor expression on the cell membrane are important to the cell's response to the binding of ligands, then gradients in extracellular voltage may be reflected in gradients of biological activity. Receptor mediated processes important to differentiation and pattern formation include recognition of cell adhesion molecules (Edelman, '85), the binding of morphogens such as the peptide growth factors of the FGF and TGF families, known to be involved in A-P specification in *Xenopus* embryos (Ruiz i Altaba and Melton, '89), and possibly endogenous retinoic acid (Maden and Holder, '91). 2) Extracellular voltage gradients can influence the shape of cells. For example myoblasts (Hinkle et al., '81), epithelial cells (Cooper and Schliwa, '85) and neural crest (Cooper and Keller, '84), as well as others (reviewed by Robinson, '85; Nuccitelli, '88; Borgens, '92), form a bipolar axis of symmetry perpendicular to the voltage gradient. Reordering of cell shape involves a re-arrangement of connections with extracellular matrix molecules and a respecification of the receptors that span the membrane and interconnect these molecules with the cytoskeleton. Such biochemical alterations do not simply reflect structural change but significantly alter the transduction of signals controlling the expression of genes important to phenotype (Ben-Ze'ev, 1991). 3) It is clear that gradients of morphogens that specifically activate or repress genes crucial to the formation of pattern exist within the egg and the multicellular embryo (Hulskamp and Tautz, '91; Melton, '91). Molecular gradients may be supported by a local source diffusion model; however, we suggest that a standing gradient of voltage can also be expected to support an asymmetrical distribution of molecules inside and outside of cells.

In the companion paper, we offer evidence suggesting the currents and fields reported here are critical to development and are not epiphenomena. If these ionic currents and their associated voltages are incidental to cell movements and the formation and definition of structure, then there would be no reason to suppose that a relatively weak (approximately 25–50 mV/mm) potential, imposed across the embryo for about 1 day, should grossly affect development. Such externally applied voltages in fact grossly interrupt normal development, and the form of developmental abnormalities at the head or tail corresponds to a particular polarity of field application (Metcalf and Borgens, this issue). Taken together, these data provide preliminary evidence for a novel electrophysiology that may help control emerging pattern in the vertebrate embryo.

ACKNOWLEDGMENTS

We acknowledge the expert technical assistance of Douglas Murphy and Debra Bohnert. We appre-

ciate Kevin Hotary's aid in 2-D probe analysis. *Xenopus* embryos were provided by Kenneth Robinson's laboratory and the axolotls by the Indiana University Axolotl Colony. We thank George Malacinski, Susan Duhon, and Sandra Borland for their diligence and care in axolotl husbandry and shipment, Michele Miller Bever and Rose Beghtol-Hunt for producing some of the graphics, Heather Eddy for manuscript preparations, and Donald Bliss for the drawings. This work is supported by a grant from the Department of Defense, DAMD17-91-Z-1008, and support of the Center for Paralysis Research from the Canadian Spinal Research Organization.

LITERATURE CITED

Armstrong, J.B., S.T. Duhon, and G.M. Malacinski (1989) Raising the axolotl in captivity. In: Developmental Biology of the Axolotl J.B. Armstrong and G.M. Malacinski eds., Oxford University Press, New York, pp. 220–227.

Barker, A.T., L.F. Jaffe, and J.W. Vanable Jr. (1982) The glabrous epidermis of cavies contains a powerful battery. Am. J. Physiol., *242:*R358–366.

Ben-Ze'ev, A. (1991) Animal cell shape changes and gene expression. BioEssays, *13:*207–212.

Bordzilovskaya, N.P., T.A. Dettlaff, S.T. Duhon, and G.M. Malacinski (1989) Developmental stage series of axolotl embryos. In: Developmental Biology of the Axolotl. J.B. Armstrong and G.M. Malacinski, eds. Oxford University Press, New York, pp. 201–219.

Borgens, R.B. (1982) What is the role of natural electric current in vertebrate regeneration and healing? Int. Rev. Cytol., *76:*245–298.

Borgens, R.B. (1984) Are limb regeneration and limb development both initiated by an integumentary wounding: A Hypothesis? Differentiation, *28:*87–93.

Borgens, R.B. (1989) Natural and applied currents in limb regeneration and development. In: Electric Fields in Vertebrate Repair, Alan R. Liss, New York, pp. 27–75.

Borgens, R.B. (1992) Applied voltages in spinal cord reconstruction: History, strategies and behavioral models. In: Spinal Cord Dysfunction III: Functional Stimulation L.S. Illis, ed. Oxford University Press, Oxford, New York, pp. 110–145.

Borgens, R.B., and C.D. McCaig (1989) Endogenous currents in nerve repair, regeneration, and development. In: Electric Fields in Vertebrate Repair, Alan R. Liss, New York, pp. 77–116.

Borgens, R.B., J.W. Vanable, Jr., and L.F. Jaffe (1977) Bioelectricity and regeneration: Large currents leave the stumps of regenerating newt limbs. Proc. Natl. Acad. Sci. U.S.A., *74:*4528–4532.

Borgens, R.B., J.W. Vanable, Jr., and L.F. Jaffe (1979a) Bioelectricity and regeneration. Bioscience, *29:*468–474.

Borgens, R.B., J.W. Vanable, Jr., and L.F. Jaffe (1979b) Reduction of sodium dependent stump currents disturbs urodele limb regeneration. J. Exp. Zool., *209:*377–386.

Borgens, R.B., M.F. Rouleau, and L.E. DeLanney (1983) A steady efflux of ionic current predicts hind limb development in the axolotl. J. Exp. Zool., *228:*491–503.

Borgens, R.B., L. Callahan, and M.F. Rouleau (1987) The anatomy of axolotl flank integument during limb bud development with special reference to a transcutaneous current predicting limb formation. J. Exp. Zool., *244:*203–214.

Cooper, M.S., and R.E. Keller (1984) Perpendicular orientation and directional migration of amphibian neural crest cells in DC electrical fields. Proc. Natl. Acad. Sci. U.S.A., *81:* 160–164.

Cooper, M.S., and M. Schliwa (1985) Electric and ionic control of tissue cell locomotion in DC electric fields. J. Neurosci. Res., *13:*223–224.

Decker, R.S. (1981) Disassembly of the zonula occludens during amphibian neurulation. Dev. Biol., *81:*12–22.

Edelman, G.M. (1985) Molecular regulation of neural morphogenesis. In: Molecular Basis of Neural Development. G.M. Edelman, W.E. Gall, and W.M. Cowan, eds. John Wiley & Sons, New York, pp. 35–60.

Erickson, C.A., and R. Nuccitelli (1984) Embryonic fibroblast motility and orientation can be influenced by physiological electric fields. J. Cell Biol., *98:*296–307.

Giugni, T.D., D.L. Braslau, and H.T. Haigler (1987) Electric field induced redistribution and post-field relation of epidermal growth factor receptors on A431 cells. J. Cell Biol, *104:*1291–1301.

Hinkle, L., C.D. McCaig, and K.R. Robinson (1981) The direction of growth of differentiating neurons and myoblasts from frog embryos in an applied electric field. J. Physiol., *314:* 121–135.

Hotary, K.B., and K.R. Robinson (1990) Endogenous electrical currents and the resultant voltage gradients in the chick embryo. Dev. Biol., *140:*149–160.

Hotary, K.B., and K.R. Robinson (1992a) A computerized 2-dimensional vibrating probe for mapping extracellular current patterns. J. Neurosci. Methods, *43:*55–67.

Hotary, K.B., and K.R. Robinson (1992b) Evidence of a role for endogenous electrical fields in chick embryo development. Development, *114:*985–996.

Hulskamp, M., and D. Tautz (1991) GAP genes and gradient—the logic behind the GAPs. BioEssays, *13:*261–266.

Jaffe, L.F. (1979) Control of development by ionic currents. In: Membrane Transduction Mechanisms. R.A. Cone and J.E. Dowling, eds. Raven Press, New York, pp. 199–229.

Jaffe, L.F. (1981) The role of ionic currents in establishing developmental pattern. Philos. Trans. R. Soc. Lond. [Biol.] *B295:*553–566.

Jaffe, L.F. (1982) Development currents, voltages, and gradients. In Developmental Order: Its Origin and Regulation S. Subtelny and P.B. Green, eds. Alan R. Liss, New York, pp. 183–215.

Jaffe, L.F., and R. Nuccitelli (1974) An ultrasensitive vibrating probe for measuring steady extracellular currents. J. Cell Biol., *63:*614–628.

Jaffe, L.F., and R. Nuccitelli (1977) Electrical controls of development. Annu. Rev. Biophys. Bioeng., *6:*445–476.

Jaffe, L.F., and C.D. Stern (1979) Strong electrical currents leave the primitive streak of chick embryos. Science, *206:* 569–571.

Kirschner, L.B. (1973) Electrolyte transport across the body surface of freshwater fish and amphibia. In: Transport Mechanisms in Epithelia. H.H. Ussing and N.A. Thorn, eds. Munksgaard, Copenhagen, pp. 447–460.

Kline, D., K.R. Robinson, and R. Nuccitelli (1983) Ion currents and membrane domains in the cleaving *Xenopus* egg. J. Cell Biol., *97:*1753–1761.

Luther, P.W., and H.B. Peng (1985) Membrane-related specializations associated with acetylcholine receptor aggregates induced by electric fields. J. Cell Biol., *100:*235–244.

Maden, M., and N. Holder (1991) Retinoic acid and development of the central nervous system. BioEssays, *14:*431–437.

McCaig, C.D. (1987) Spinal neurite reabsorption and regrowth in vitro depend on the polarity of an applied electric field. Development, *100:*31–41.

McCaig, C.D., and K.R. Robinson (1982) The ontogeny of the transepidermal potential difference in frog embryos. Dev. Biol., *90:*335–339.

McGinnis, M.E., and J.W. Vanable Jr. (1986) Electrical fields in *Notophthalmus viridescens* limb stumps. Dev. Biol., *116:*184–193.

Melton, D.A. (1991) Pattern formation during animal development. Science, *252:*234–241.

Metcalf, M.E.M., and R.B. Borgens (1994) Weak applied voltages interfere with amphibian morphogenesis and pattern. J. Exp. Zool., *268:*323–338.

Nieuwkoop, P.D., and J. Faber (1956) Normal Table of *Xenopus Laevis* (Daudin). North-Holland Publishing Co.,Amsterdam.

Nuccitelli, R. (1986) A two-dimensional vibrating probe with a computer graphics display. In: Ionic Currents in Development. Alan R. Liss, New York, pp. 13–20.

Nuccitelli, R. (1988) Physiological electric fields can influence cell motility, growth and polarity. Adv. Cell Biol., *2:*213–233.

Nuccitelli, R., and C.A. Erickson (1983) Embryonic cell motility can be guided by physiological electrical fields. Exp. Cell Res., *147:*195–201.

Orida, N., and J.D. Feldman (1982) Directional protrusive pseudopodial activity and motility in macrophages induced by extracellular electric fields. Cell Motil. *2:*243–255.

Poo, M.-M, and K.R. Robinson (1977) Electrophoresis of concanavalin A receptors along embryonic muscle cell membrane. Nature, *265:*602–605.

Robinson, K.R. (1983) Endogenous electrical current leaves the limb and prelimb region of the *Xenopus* embryo. Dev. Biol., *97:*203–211.

Robinson, K.R. (1985) The responses of cells to electrical fields: J. Cell Biol., *101:*2023–2027.

Robinson, K.R., and R.F. Stump (1984) Self-generated electrical currents through *Xenopus* neurulae. J. Physiol., *352:* 339–352.

Ruiz i Altaba, A., and D.A. Melton (1989) Interaction between peptide growth factors and homeobox genes in the establishment of antero-posterior polarity in frog embryos. Nature, *341:*33–36.

Sariban-Sohraby, S., and D.J. Benos (1986) The amiloride-sensitive sodium channel. Am. J. Physiol., *250:*C175–C190.

Stump, R.F., and K.R. Robinson (1983) *Xenopus* neural crest cell migration in an applied electrical field. J. Cell Biol., *97:*1226–1233.

Tank, D.W., W.J. Fredericks, L.S. Barak, and W.W. Webb (1985) Electric field–induced redistribution and post-field relaxation of low density lipoprotein receptors on cultured human fibroblasts. J. Cell Biol., *101:*148–161.

Vanable, J.W., Jr. (1989) Integumentary potentials and wound healing. In: Electric Fields in Vertebrate Repair. Alan R. Liss, New York, pp. 171–224.

Winkle, G.K., and R. Nuccitelli (1989) Large ionic currents leave the primitive streak of the 7.5-day mouse embryo. Bio. Bull., *176(S):*110–117.

Zagyansky, Y.A., and S. Jard (1979) Does lectin-receptor complex formation produce zones of restricted mobility within the membrane? Nature, *280:*591–593.